DNA Ligase III as a Candidate Component of Backup Pathways of Nonhomologous End Joining

Huichen Wang,[1] Bustanur Rosidi,[2] Ronel Perrault,[1] Minli Wang,[2] Lihua Zhang,[2] Frank Windhofer,[2] and George Iliakis[1,2]

[1]Department of Radiation Oncology, Division of Experimental Radiation Oncology, Kimmel Cancer Center, Jefferson Medical College, Philadelphia, Pennsylvania and [2]Institute of Medical Radiation Biology, University Duisburg-Essen Medical School, Essen, Germany

Abstract

Biochemical and genetic studies support the view that the majority of DNA double-strand breaks induced in the genome of higher eukaryotes by ionizing radiation are removed by two pathways of nonhomologous end joining (NHEJ) termed D-NHEJ and B-NHEJ. Whereas D-NHEJ depends on the activities of the DNA-dependent protein kinase and DNA ligase IV/XRCC4, components of B-NHEJ have not been identified. Using extract fractionation, we show that the majority of DNA end joining activity in extracts of HeLa cells derives from DNA ligase III. DNA ligase III fractionates through two columns with the maximum in DNA end joining activity and its depletion from the extract causes loss of activity that can be recovered by the addition of purified enzyme. The same fractionation protocols provide evidence for an additional factor strongly enhancing DNA end joining and shifting the product spectrum from circles to multimers. An *in vivo* plasmid assay shows that DNA ligase IV–deficient mouse embryo fibroblasts retain significant DNA end joining activity that can be reduced by up to 80% by knocking down DNA ligase III using RNA interference. These *in vivo* and *in vitro* observations identify DNA ligase III as a candidate component for B-NHEJ and point to additional factors contributing to NHEJ efficiency. (Cancer Res 2005; 65(10): 4020-30)

Introduction

Endogenous cellular processes and exogenous factors such as ionizing radiation generate double-strand breaks (DSB) in the DNA that undermine genomic integrity. Three enzymatically distinct processes, homology-directed repair, single-strand annealing, and nonhomologous end joining (NHEJ) can, in principle, repair DNA DSBs (1–4). In cells of higher eukaryotes, repair of ionizing radiation–induced DNA DSBs is dominated by NHEJ, which as a first approximation can be classified in two pathways. The first pathway, DNA-dependent protein kinase (DNA-PK)–dependent NHEJ (D-NHEJ), is responsible for a large proportion of the fast component of rejoining observed in wild-type cells and requires the activities of DNA-PK and DNA ligase IV/XRCC4. The second component, backup NHEJ (B-NHEJ), corresponds to the slow rejoining observed in wild-type cells, as well as to the majority of end joining in cells with defects in factors required for D-NHEJ and is supported by as of yet unidentified factors (5–7).

Recent biochemical studies focus on the coordination between these pathways of NHEJ using as a model *in vitro* end joining by cell extracts of restriction endonuclease–linearized plasmid DNA. Efficient DNA end joining can be observed *in vitro*, which is inhibited by anti-Ku antibodies if DNA-PKcs is present (5). Strong inhibition of DNA end joining is also mediated by wortmannin, an inhibitor of DNA-PKcs, in the presence but not in the absence of Ku (5, 7). These results suggest that Ku and DNA-PKcs act in a coordinated manner to direct end joining to a DNA-PK–dependent pathway. On the other hand, efficient end joining is observed in extracts of cells lacking DNA-PKcs, as well as in Ku-depleted extracts in line with the operation of alternative pathways equivalent to B-NHEJ (5, 7). It is thus conceivable that *in vivo*, DNA ends are quickly captured by Ku cooperating with DNA-PKcs and are directed to D-NHEJ for rapid joining, kinetically suppressing thus slower backup pathways such as B-NHEJ (5). Alternative pathways of end joining such as B-NHEJ are expected to contribute significantly to the overall repair of DNA DSBs when components of D-NHEJ are either absent from the vicinity of the break, or genetically/chemically compromised, and may therefore contribute to genome maintenance and stability. Evidence *in vivo* and *in vitro* suggests that backup pathways of NHEJ are error prone, and that this characteristic is the cause of translocations leading to tumor induction in mice with defects in D-NHEJ (8–12).

Despite the significance of backup pathways such as B-NHEJ in the repair of DNA DSBs and genomic stability, information on the factors involved is lacking. Here we report biochemical studies designed to characterize components of B-NHEJ. Using extract fractionation, we show that the majority of end joining activity in extracts of HeLa cells derives from DNA ligase III. The same fractionation protocols provide evidence for additional factors enhancing end joining. These observations and *in vivo* plasmid end joining results point to DNA ligase III as a candidate component of B-NHEJ.

Materials and Methods

Cell lines and extract preparation. HeLa cells were grown either as monolayer or suspension cultures in Joklik's modified MEM (S-MEM) supplemented with 5% bovine calf serum. 180BRM is a cell line derived in our laboratory from 180BR primary fibroblasts by transfection with plasmid pRNS-1 containing a replication deficient form of SV40 virus and the *neo* gene that confers resistance to G418 (70 μg/mL). 180BRM cells have an extended life span that allows maintenance in culture under active growth for several months (30-40 passages) but are not truly immortalized. Primary 180BR fibroblasts were established from a patient with acute lymphoblastic leukemia who died from radiation morbidity (13). The cells carry a homozygous, hypomorphic mutation in DNA ligase IV causing the

Note: H. Wang and B. Rosidi contributed equally to the work.

H. Wang is currently at the Center for Neurovirology and Cancer Biology, College of Science and Technology, Temple University, 1900 North 12th Street, 015-96, Philadelphia, PA 19122.

R. Perrault is currently at the Department of Microbiology and Immunology, Drexel University College of Medicine, Philadelphia, PA 19129.

Requests for reprints: George Iliakis, Institute of Medical Radiation Biology, University Duisburg-Essen Medical School, Hufelandstr. 55, 45122 Essen, Germany. Phone: 49-201-723-4152; Fax: 49-201-723-5966; E-mail: georg.iliakis@uni-essen.de.

substitution of His^{278} for arginine (R278H) within a motif close to the conserved active lysine site (14, 15). Although this mutation does not confer a null phenotype, 180BR cells are radiosensitive to killing and defective in the repair of DNA DSB (16). 180BRM cells were grown as monolayer in MEM supplemented with 10% bovine calf serum. Mouse embryo fibroblasts (MEF) from $LIG4^{-/-}/p53^{-/-}$ animals (called here as $LIG4^{-/-}$ MEF; 17) were grown in DMEM supplemented with 10% fetal bovine serum and antibiotics.

Experiments were done either with whole cell extract (WCE) or with nuclear extract. For the preparation of HeLa cell extracts a 1- to 30-liter suspension of cells was grown in spinner flasks to 0.5 to 1×10^6 cells/mL and collected by centrifugation. For 180BRM extract preparation, 100 dishes (100 mm, 20 mL growth medium, 0.5×10^6 cells) were prepared and cells were allowed to grow up to $\sim 5 \times 10^6$ cells per dish before harvesting by trypsinization. For further processing, cells from both cell lines were washed once in ice-cold PBS and subsequently in five packed cell volumes of cold hypotonic buffer [10 mmol/L HEPES (pH 7.5), 5 mmol/L KCl, 1.5 mmol/L $MgCl_2$, 0.2 mmol/L phenylmethylsulfonyl fluoride (PMSF), and 0.5 mmol/L DTT]. The cell pellet was resuspended in two volumes of hypotonic buffer and after 10 minutes in ice, disrupted in a Dounce homogenizer (15 strokes with a "B" pestle). For the preparation of WCE, 3 mol/L KCl were slowly added to the homogenate to a final concentration of 0.5 mol/L KCl and after 30 minutes on ice, centrifuged for 40 minutes at 14,000 rpm at 4°C. To remove DNA from the extract, one tenth extract volume of DEAE Sepharose, equilibrated in dialysis buffer [25 mmol/L HEPES (pH 7.5), 100 mmol/L KCl, 1 mmol/L EDTA, 10% glycerol, 0.2 mmol/L PMSF, and 0.5 mmol/L DTT], was added and the mixture was gently rotated at 4°C for 30 minutes. Extract was cleared by centrifugation at 12,000 rpm for 20 minutes and dialyzed overnight in dialysis buffer. After centrifugation, aliquots of the extract were snap frozen and stored at −80°C.

For nuclear extract preparation, cells were homogenized as above and 3 mol/L KCl were slowly added to a final concentration of 50 mmol/L KCl. The extract was incubated for 10 minutes on ice and centrifuged for 30 minutes at $3{,}300 \times g$ at 4°C. Supernatant was collected as cytoplasmic extract. Nuclear pellet was resuspended in two packed nuclear volumes (pnv) of low salt buffer [20 mmol/L HEPES (pH 7.9), 20 mmol/L KCl, 1.5 mmol/L $MgCl_2$, 0.2 mmol/L EDTA, 0.2 mmol/L PMSF, and 0.5 mmol/L DTT] and 1 pnv of high salt buffer [10 mmol/L HEPES (pH 7.5), 1.6 mol/L KCl, and 1.5 mmol/L $MgCl_2$] was slowly added to a final concentration of 400 mmol/L KCl. Extract was incubated for 30 minutes at 4°C under gentle shaking and centrifuged for 30 minutes at $50{,}000 \times g$ at 4°C. The supernatant was collected as nuclear extract. In some preparations of nuclear extract, DEAE Sepharose (0.1 volume) was added to remove DNA as described above for WCE, and subsequently nuclear extract was dialyzed overnight in dialysis buffer [20 mmol/L HEPES (pH 7.9), 10% to 20% glycerol, 100 mmol/L KCl, 0.2 mmol/L EDTA, 0.2 mmol/L PMSF, and 0.5 mmol/L DTT] before aliquoting, snap freezing, and storing at −80°C.

In a series of experiments designed to optimize end joining in nuclear extract, we observed extensive protein precipitation and loss of DNA end joining activity after dialysis in buffer containing 100 mmol/L KCl (see above), particularly when extract concentration was relatively high (3-6 mg/mL). This adverse effect was practically eliminated by dialyzing against 400 mM KCl, which was therefore adopted as routine preparation procedure in later experiments. Extracts prepared under these conditions are designated nuclear extract/high salt to indicate their dialysis against a high salt buffer. Finally, because DNA end joining activity remained partially bound on DEAE Sepharose used to remove DNA from nuclear extract, we chose to omit this step in more recent extract preparations. The outlined modifications resulted in quantitative rather than qualitative improvements in extract preparation and, with this in mind, results obtained using early or late preparations of extract can be compared with each other.

Extract fractionation. Fractionation of DNA end joining factors was achieved over a dsDNA-cellulose (Sigma, St. Louis, MO) followed by a Mono-S (Amersham Biosciences, Piscataway, NJ) column. Initial fractionations on dsDNA cellulose (5-10 mL volume, D = 1.6 cm) were carried out using 20 to 30 mL nuclear extract (50-150 mg) loaded at a flow rate of 0.5 mL/min after equilibration with buffer A [20 mmol/L HEPES (pH 7.9), 10% glycerol, 0.2 mmol/L EDTA, 0.2 mmol/L PMSF, and 0.5 mmol/L DTT] containing 100 mmol/L KCl. In addition to the flow through (peak I), fractions were collected after increasing, stepwise, KCl concentration to 250 mmol/L (peak II) and 750 mmol/L (peak III). Because the vast majority of activity bound the column and eluted in the 750 mmol/L step (peak III), later fractionations using nuclear extract/high salt that was dialyzed against 400 mmol/L KCl to preserve activity (see above), were initiated by diluting nuclear extract/high salt with buffer A to 300 mmol/L KCl and loading to dsDNA cellulose column after equilibration at the same concentration of KCl. The flow through obtained under these conditions was designated peak I/II to maintain previous nomenclature. DNA end joining activity was again predominantly eluted at 750 mmol/L KCl (peak III). The end joining activity obtained with these two protocols was qualitatively equivalent, but quantitatively more overall activity was recovered with the latter protocol due to the higher initial activity of the nuclear extract/high salt.

Active fractions of peak III were pooled and dialyzed against buffer A containing 100 mmol/L KCl and loaded, at a flow rate of 0.5 mL/min, onto a 1 mL Mono S HR 5/5 column equilibrated in the same buffer. A linear gradient over 10 column volumes was applied up to 300 mmol/L KCl, followed by three stepwise increases to 500, 700, and 1,000 mmol/L KCl, each over 5 to 10 column volumes. Fractions obtained from all fractionation steps were tested for protein concentration using the Bradford assay (Bio-Rad, Hercules, CA), and for *in vitro* DNA end joining activity (see below).

Proteins and antibodies. Antibodies against DNA ligase III, clones 1F3, 4C11, 6G9, and a mouse polyclonal were from GeneTex (San Antonio, TX); a rabbit polyclonal antibody against DNA ligase IV, raised against the COOH-terminal residues 550 to 844, from Acris (Hiddenhausen, Germany); a mouse monoclonal antibody against DNA ligase I, clone 10H5, from GeneTex; a mouse monoclonal antibody against Ku70, clone N3H10, from Kamiya Biomedical Co. (Seattle, WA); a mouse monoclonal antibody against Ku80, clone 111, from Kamiya Biomedical; a rabbit polyclonal antibody against DNA-PKcs, raised by an 11 residue synthetic peptide, from Calbiochem (La Jolla, CA); a rabbit polyclonal antibody, raised against the full length human XRCC4, from Acris; a mouse monoclonal antibody against PARP-1, clone C2-10, was from Sigma; and a mouse monoclonal antibody against XRCC1, clone 33-2-5, from Abcam (Cambridge, United Kingdom).

Western blot analysis and immunodepletion. For Western blot, cell extracts were electrophoresed on 10% SDS-polyacrylamide gels, transferred to a polyvinylidene difluoride membrane, and probed by the enhanced chemiluminescence-Plus kit as recommended by the manufacturer (Amersham Biosciences). Signal was detected using the "Storm," the "Typhoon" (Amersham Biosciences), or the VersaDoc (Bio-Rad).

For DNA ligase III immunodepletion, 20 μL of anti DNA ligase III antibody, or normal human serum were added to 50 μL of protein A-Sepharose beads in 250 μL of DB buffer [20 mmol/L HEPES (pH 7.9), 100 mmol/L KCl, 20% glycerol, 0.2 mmol/L EDTA, 0.5 mmol/L DTT, and 0.5 mmol/L PMSF] with 50 μg/mL bovine serum albumin (18). Mixture was incubated under constant rotation at 4°C overnight. Subsequently, beads were washed thrice with dialysis buffer, and incubated with 100 to 200 μL HeLa or 180BRM WCE for 2 hours at 4°C. After centrifugation, the supernatants were used for quantification of depletion and DNA end joining, whereas the beads were washed thrice with dialysis buffer before analysis by Western blotting. When necessary, additional depletion cycles were carried out until depletion was nearly complete.

DNA end joining and DNA ligase assays. Supercoiled plasmid pSP65 (3 kb; Promega, Madison, WI) was prepared using $CsCl_2$/EtBr gradients. It was used as a substrate in DNA end joining reactions following digestion with *Sal*I to generate linearized DNA. Details have been presented elsewhere (5, 7). DNA ligase III activity was measured according to published protocols with slight modifications (19). DNA ligase IIIβ was purified using methods and constructs as previously described (20).

Digestion of DNA end joining products with nuclease S1. In some experiments, products of the end joining reaction were digested with Nuclease S1 from *Aspergillus oryzae* (EC 3.1.30.1; Roche, Nutley, NJ). DNA

was incubated at 37°C for 30 minutes with the indicated amount of nuclease S1 in a buffer containing 33 mmol/L sodium acetate, 50 mmol/L NaCl, and 0.033 mmol/L $ZnSO_4$ (pH 4.5). Under these reaction conditions, nuclease S1 exerts exonucleolytic and endonucleolytic activity on ssDNA.

***In vivo* DNA end joining.** To document a role for DNA ligase III in DNA end joining *in vivo*, we employed a recently developed fast-readout plasmid-rejoining assay using the plasmid pEGFP-Pem1-Ad2 (21). The plasmid is a derivative of pEGFP-Pem1 (7,139 bp) that was generated by L. Li from pEGFP-N1 (Clontech, Palo Alto, CA) by interrupting the enhanced green fluorescent protein (EGFP) sequence with the Pem1 intron. It was constructed by inserting the wild-type adenoviral major late mRNA leader sequence (adenoviral exon 2, Ad2) into the polylinker site within the Pem1 intron of pEGFP-Pem1 after appropriate modifications to generate *Hin*dIII and *I-Sce*I cutting sites, as well as splice sites on both sides of Ad2 (Fig. 6). In this configuration, the EGFP gene is normally disrupted by the Ad2 exon and therefore transfection of supercoiled plasmid generates no EGFP signal. When Ad2 is removed before transfection by digestion at both sides either with *Hin*dIII or *I-Sce*I, EGFP activity can be recovered if the transfected cell possesses end joining activity to recircularize the linear plasmid. Partly digested plasmid that retains the Ad2 sequence generates no signal. In experiments reported here, the pEGFP-Pem1-Ad2 plasmid was digested with *Hin*dIII to remove Ad2 and generate cohesive ends with 4-bp 5′ protruding single strands. Supercoiled pEGFP-Pem1 was used as a positive control to standardize the transfection and analysis conditions. The pDsRed2-N1 plasmid (Clontech) was cotransfected with either linearized pEGFP-Pem1-Ad2 or supercoiled pEGFP-Pem1 to evaluate the transfection efficiency. All plasmids were prepared in XL-1 blue cells and purified using either $CsCl_2$/EtBr gradients, or the Qiagen Midi Plasmid purification kit. The *Hin*dIII linearized pEGFP-Pem1-Ad2 was purified by gel electrophoresis to remove the Ad2 fragment.

Plasmid rejoining was tested in *LIG4*$^{-/-}$ MEF. The appropriate plasmids were transfected using the MEF1 nucleofector kit in the Nucleofector devise (Amaxa, Cologne, Germany) according to the instructions of the manufacturer. Typically, a suspension of 2×10^6 cells was transfected by electroporation with 0.2 μg pEGFP-Pem1, or *Hin*dIII linearized pEGFP-Pem1-Ad2 substrate, together with 0.2 μg of the transfection efficiency marker pDsRed2-N1. Green (EGFP) and Red (DsRed) fluorescence were measured by flow cytometry 24 hours later. For this purpose, cells were trypsinized and resuspended in fresh growth medium at 10^6 per mL. Analysis was carried out in a Beckman Coulter Epics XL-MCL flow cytometer equipped with an argon ion laser emitting at 488 nm. Red fluorescence was collected at 540 nm with 740 V PMT gain, whereas green fluorescence at 490 nm with 490V PMT gain. Electronic compensation was 12.8% of green signal for red and 6.7% of red signal for green. Transfection with supercoiled pEGFP-Pem1 was used to calibrate the system. To include the transfection efficiency in the calculation of percent rejoining the $EGFP^+/dsRed^+$ ratio was calculated and compared between treated and nontreated cells. Results have been confirmed in three or more independent experiments.

DNA ligase III knock down. RNA interference (RNAi) mediated by small interfering RNAs (siRNA) was used to knock down DNA ligase III (*LIG3*) in *LIG4*$^{-/-}$ MEF. For this purpose, the sequences S1, GGAACAGATAAGCCAGCAT (522 nucleotides downstream); S2, GCACAAAGATTGTCTGCTA (774 nucleotides downstream); S3, GGATGTGAAGGGTACATAT (1,989 nucleotides downstream), as well as the unique negative control duplex (OR-0030-neg05) were synthesized (Eurogentec, Ouree, Belgium) and tested by transfection with electroporation under the conditions described above using 5×10^6 cells and 10 μg *LIG3* or control siRNA per transfection reaction. After transfection, cells were returned to normal growth conditions and the level of knock down evaluated at the indicated times by Western blotting. Whereas all sequences tested showed knock down activity, S2 was the most effective and was therefore primarily employed in further experiments. To test the effect of DNA ligase III knock down on DNA DSB repair, siRNA-treated cells were transfected with test and control plasmids as described above and rejoining efficiency was measured 24 hours later.

Results

Fractionation of DNA end joining activities from nuclear extract. In the course of the experiments described here, we observed loss of DNA end joining activity in the extracts which, we suspected, it was caused by protein precipitation during the last dialysis step of the standard preparation protocol (see Materials and Methods). Figure 1*A* shows that nondialyzed nuclear extract has a much higher DNA end joining activity than the same extract after dialysis against 100 mmol/L KCl. In fact, the activity measured with 2 μg nondialyzed nuclear extract is approximately equivalent to that of 10 μg nuclear extract dialyzed against 100 mmol/L KCl. Importantly, when extract was dialyzed against 400 mmol/L KCl, a practically complete preservation of end joining activity was achieved. We observed that this modification in the dialysis conditions minimizes protein precipitation and thus maximizes the preservation of DNA end joining activity. This is illustrated by the Western blot for DNA ligase III shown in the top part of the figure. Nondialyzed nuclear extract and nuclear extract dialyzed against 400 mmol/L KCl have equivalent amounts of DNA ligase III. Nuclear extract dialyzed against 100 mmol/L KCl, on the other hand, has much reduced DNA ligase III levels, and a large amount of DNA ligase III can be found with the precipitated material. Dialysis is important for the retention of activity in the extracts during storage at −80°C. Below, experiments of earlier date use extracts (WCE or nuclear extract) prepared according to the standard protocol; whereas recent experiments use nuclear extract dialyzed against 400 mmol/L KCl (nuclear extract/high salt).

The goal of the present studies was the development of appropriate fractionation strategies for the purification and characterization of factors involved in DNA end joining. We reasoned that proteins involved in DNA end joining are likely to bind to DNA and tested therefore dsDNA cellulose, because preliminary experiments showed strong binding to this resin of DNA end joining factors. A fractionation scheme was developed for nuclear extract prepared under standard conditions that involves loading at 100 mmol/L KCl (flow through; peak I) and elution at 250 mmol/L (peak II) and 750 mmol/L (peak III) KCl. For the fractionation of nuclear extract/high salt, KCl concentration in the extract is reduced to 300 mmol/L by dilution with buffer before loading, generating the combined peak I/II as flow through and peak III by elution at 750 mmol/L KCl (Fig. 1*B* and *C*). Under all conditions, the majority of DNA end joining activity is recovered in the fractions of peak III (Fig. 1*D*; data not shown), which is therefore used for further fractionation. Fractions from peaks I, II, or I/II, alone or in combination with fractions from peak III, do not produce more than additive effects (data not shown), suggesting that peak III contains the essential DNA end joining factors. Because fraction III contains only about 3% of the input protein (Fig. 1*B*), the scheme achieves a high degree of fractionation of DNA end joining activities.

Protein from active fractions of peak III was dialyzed, loaded on Mono-S, and eluted according to the scheme shown in Fig. 1*B*. Figure 2*A* shows a typical chromatogram. In addition to the flow-through peak IIIA, protein peaks IIIB1 and IIIB2 elute within the 100 to 300 mmol/L KCl gradient, and peaks IIIC and IIID at the 500 and 700 mmol/L KCl steps, respectively. Peaks IIIA and IIIC do not contain DNA end joining activities, either when tested alone or when combined with other active fractions (data not shown). Peak IIIB1 shows a very low level of activity, whereas peak IIIB2 is very active (Fig. 2*B*). Fraction IIID is not active when tested alone

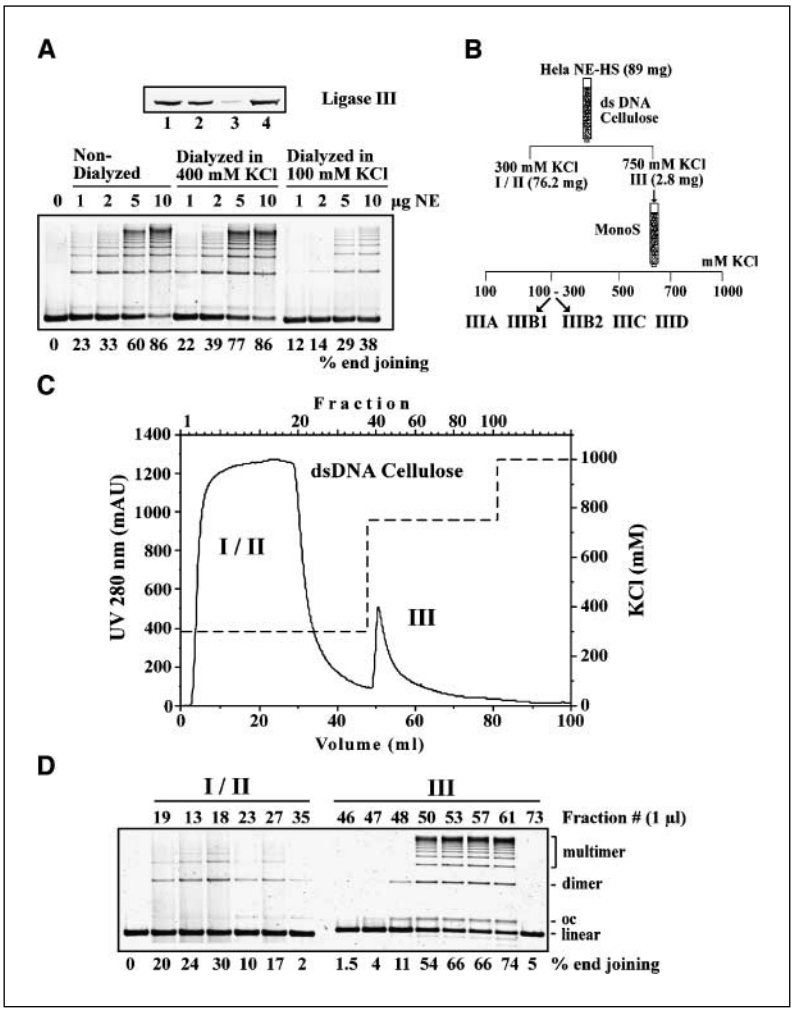

Figure 1. Extract preparation conditions and fractionation over dsDNA cellulose. *A,* DNA end joining activity in reactions assembled with different amounts of nondialyzed nuclear extract (*NE*), as well as of extract dialyzed against either 400 or 100 mmol/L KCl. Nuclear extract was prepared by treatment of nuclei in 400 mmol/L KCl, and dialysis was carried out overnight in a buffer containing the indicated amounts of KCl (see Materials and Methods for details). The numbers at the bottom of the gel indicate percent end joining. *Top,* Western blot for DNA ligase III of the same extract preparations. *Lane 1,* nondialyzed nuclear extract; *lane 2,* nuclear extract dialyzed against 400 mmol/L KCl; *lane 3,* nuclear extract dialyzed against 100 mmol/L KCl; *lane 4,* precipitated material after dialysis of nuclear extract in 100 mmol/L KCl. *B,* fractionation scheme of nuclear extracts (nuclear extract/high salt, *NE-HS*) over dsDNA cellulose followed by further fractionation of active fractions (*fraction III*) over Mono S. The scheme indicates the conditions used to generate the designated fractions and shows in brackets the amount of protein in selected fractions from a typical experiment. *C,* typical chromatogramme (absorption versus fraction number) of nuclear extract/high salt fractionated over dsDNA cellulose. The dashed line shows the steps in KCl concentration employed to generate the indicated fractions (fraction sizes: FT 1.5 mL and eluted fractions 0.5 mL). *D,* DNA end joining activity of fractions I/II and III. Reactions were assembled with 1 μL of the indicated fraction. Numbers at the top of the gel indicate tested fractions, whereas those at the bottom of the gel the percent end joining measured. The difference in activity between flow through fraction I/II and fraction III is even greater when reactions are assembled with smaller volumes of the individual fractions. Input linear substrate, as well as dimers and multimers produced by end joining. Position of the relaxed plasmid (*oc*). Based on our observations (see nuclease S1 results in Fig. 5), this product does not correspond to nicked plasmid, but rather to a covalently closed yet not supercoiled form.

(Fig. 2*B*). However, when fraction IIID is combined with fractions of IIIB1 and particularly of IIIB2 peak an enhancement in DNA end joining activity is observed (Fig. 2*C*). Notably, when combined with IIIB2, end joining activity increases steadily up to 0.5 μL IIID but drops sharply at higher concentrations suggesting that the active factor(s) in IIID has an optimum in its mode of action (Fig. 2*C*).

SDS-PAGE and Western blotting were carried out in an effort to identify candidates for the activity observed in the above fractions and the results are summarized in Fig. 3*A* and *B*. A few dominant bands are visible in fractions IIIB1 and IIIB2, but only two or three prominent bands are seen in IIID (Fig. 3*A*). Western blot analysis for the three known ligases and the components of DNA-PK show that DNA ligase I fractionates practically exclusively in peak I/II (Fig. 3*B*). DNA ligase III fractionates from dsDNA cellulose practically exclusively in fraction III and from Mono-S in fraction IIIB2. The bulk of DNA ligase IV and XRCC4 is in dsDNA cellulose fraction I/II, but a considerable amount also binds the resin and elutes with fraction III; from Mono-S these proteins fractionate preferentially in IIIB1. Similar fractionation characteristics are also observed for DNA-PKcs. The majority of Ku70/Ku80 is, as expected, in fraction III, and shows preferential fractionation from Mono-S in IIIB1. On the other hand, PARP-1 and XRCC1 fractionate preferentially in IIIB2. Thus, all major components of D-NHEJ, DNA-PKcs, Ku, DNA ligase IV, and XRCC4, elute preferentially from Mono-S in IIIB1. The low amounts of activity observed in this fraction despite the presence of all these factors is consistent with the previously shown requirement for additional factors for efficient end joining (22–24). Notably, the majority of DNA end joining activity fractionates in IIIB2 together with DNA ligase III, PARP-1, and XRCC1.

DNA ligase III is involved in DNA end joining. The above fractionation and precipitation data implicate DNA ligase III in DNA end joining. To evaluate further a possible role for this ligase in DNA end joining, we studied the effect of antibodies raised against this protein in nonfractionated HeLa cell extracts. In contrast to reactions assembled with increasing amount of nonspecific immunoglobulin G or PBS (PBS data not shown), reactions assembled with the DNA ligase III–specific monoclonal antibodies 4C11, and 1F3 show substantial inhibition of DNA end joining with increasing antibody concentration (Fig. 4*A*). In addition, a mouse polyclonal antibody (pAb) shows a strong inhibition of DNA end joining (Fig. 4*A*). The strong and at times complete inhibition achieved with three different antibodies suggests a dominant role for DNA ligase III in DNA end joining under the reaction conditions employed here. On the other hand, the anti DNA ligase III monoclonal antibody 6G9 has no detectable effect on DNA end joining suggesting that the inhibition depends on the location of the epitope recognized by the antibody.

Similar results were also obtained in reactions assembled with extracts prepared from 180BRM cells. Although these cells have reduced DNA ligase IV activity, they show nearly normal DNA end joining activity under the *in vitro* conditions employed here and are therefore a useful system for the evaluation of a possible effect DNA ligase III on DNA end joining because they reduce interference from DNA ligase IV (25). Figure 4*B* shows that the mouse polyclonal anti–DNA ligase III antibody inhibits, practically completely, end joining in reactions assembled with WCE of 180BRM cells. An antibody against DNA ligase I (26) and a control antibody (mIgG) show no effect on DNA end joining (Fig. 4*B*).

To confirm the role of DNA ligase III in DNA end joining, we immunodepleted DNA ligase III from WCE of HeLa and 180BRM cells using the mouse polyclonal antibody pAb. Figure 4*C* shows that DNA ligase III is undetectable in immunodepleted extracts of 180BRM cells, and Fig. 4*D* shows that DNA end joining is barely detectable in these extracts. To establish that depletion of DNA ligase III is the reason for DNA end joining activity loss, purified DNA ligase IIIβ was added back to the reactions. Although, this form of DNA ligase III lacks the COOH-terminal BRCT domain and is therefore unable to interact with XRCC1, it has been shown to effectively substitute for DNA ligase IIIα in several assays (27). The purity of the enzyme used is shown in Fig. 4*E*. Figure 4*F* shows that added DNA ligase IIIβ in immunodepleted extracts of 180BRM cells completely restores DNA end joining activity. Although purified DNA ligase IIIβ by itself shows end joining activity, the spectrum of products strongly shifts from open and supercoiled rings to linear multimers in DNA ligase III supplemented extracts. Similar results were also obtained with immunodepleted extracts of HeLa cells (see Fig. 4*C* and *D*), although the inhibition of DNA end joining was in this case less pronounced, probably due to the presence in the extracts in addition to DNA ligase IV also of residual DNA ligase III (see Fig. 4*C*).

DNA ligase III joins both DNA strands practically simultaneously. In the end joining assay employed here, open circles and multimers can be formed by joining only one strand of the participating double-stranded plasmid DNA molecules. It is, therefore, formally possible that the activity actually measured reflects single rather than double strand DNA joining, an activity commonly attributed to DNA ligase III (28–30). We exploited the properties of nuclease S1 to test this possibility. Nuclease S1 is known to endonucleolytically and exonucleolytically digest ssDNA, and to preferentially cut double-stranded DNA opposite nick sites. We reasoned that if open circles and polymers produced in the end joining reaction derive from single-strand ligation, treatment with nuclease S1 should be able to digest opposite the remaining nick and regenerate the original substrate. If, on the other hand, open circles and polymers are generated by the joining of both DNA

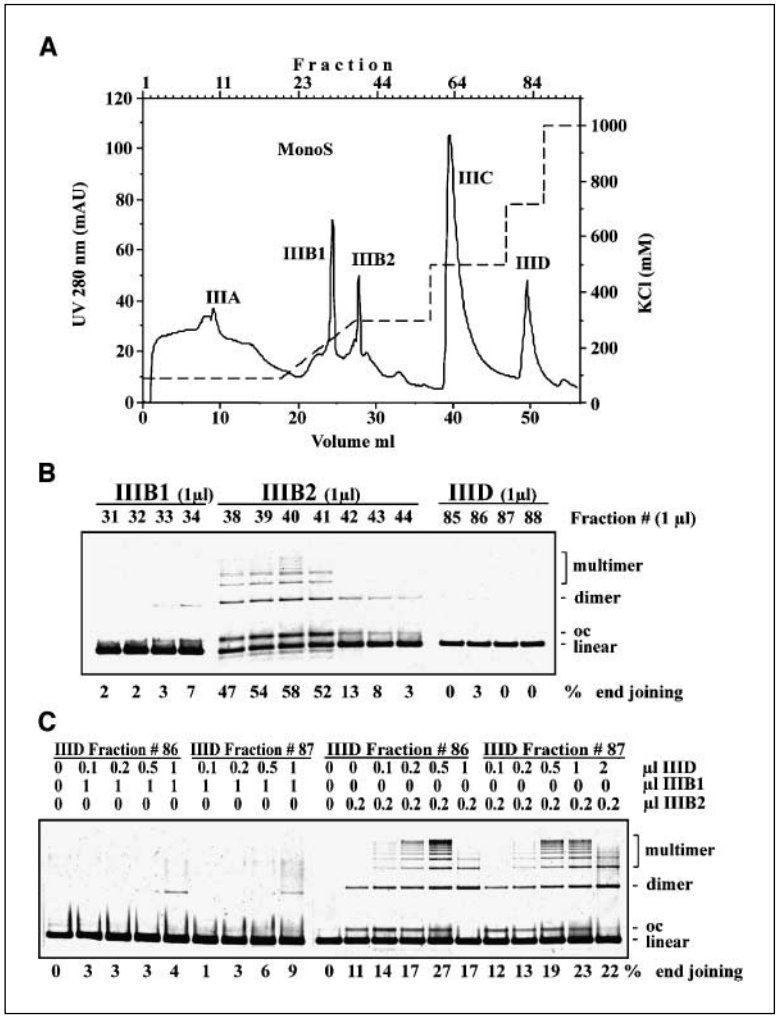

Figure 2. Fractionation of DNA end joining activities over Mono S. *A,* typical chromatogramme of fractionation through Mono S of fraction III from dsDNA cellulose. The dashed line shows the steps in KCl concentration employed to generate the indicated fractions. *B,* DNA end joining activity of the indicated fractions from Mono S. Reactions were assembled with 1 μL of the indicated fraction. Numbers at the top of the gel indicate tested fractions, whereas those at the bottom of the gel the percent end joining measured. *C,* peak fractions IIIB1 (1 μL) and IIIB2 (0.2 μL) were tested for DNA end joining in reactions assembled with increasing amount of IIID (0.1-2 μL). Numbers at the top of the gel indicate tested fractions, whereas those at the bottom of the gel the percent end joining measured. Other details as in Fig. 1.

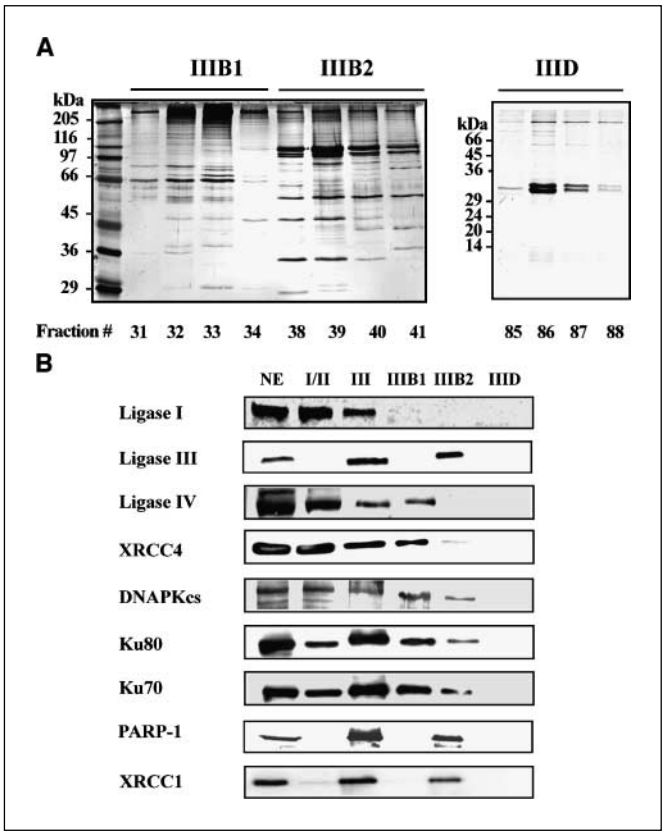

Figure 3. Analysis by SDS-PAGE and Western blotting of active fraction from Mono S. *A,* SDS PAGE of indicated fractions surrounding peaks IIIB1 and IIIB2. For IIIB1 and IIIB2 lanes, 10 μL aliquots of each fraction were used and the gel (10%) was stained with silver. For IIID 20 μL aliquots of the indicated fractions were used and the gel (15%) was stained with Coomassie. *B,* Western blots of peak fractions of dsDNA cellulose and Mono S using antibodies against the indicated proteins. See Materials and Methods for details.

strands, products of the reaction should show sensitivity to nuclease S1 similar to that of the unligated substrate.

Figure 5*A* shows the substrate specificity of nuclease S1 under the conditions employed. *Sal*I-linearized plasmid DNA used as substrate in the end joining reactions remains resistant to digestion up to 1 unit of enzyme. At higher levels of S1 activity, nonspecific digestion is observed giving rise to a low molecular weight smear. Supercoiled plasmid, on the other hand, is efficiently converted to the relaxed form at levels of S1 activity as low as 0.01 unit, presumably by endonucleolytic digestion at single-stranded areas transiently generated by negative supercoiling. Following this initial step that leads to the relaxation of the plasmid, a second specific cut opposite the nick generates linear molecules of substrate size at enzyme concentrations up to 1 unit per reaction. At higher enzyme concentrations nonspecific digestion occurs generating a low molecular weight smear. Similar results were also obtained when the relaxed form of pSP65 was purified and used as S1 substrate (data not shown). The above observations confirm the expected specificity of nuclease S1 under our reaction conditions and serve as a positive control for the following reactions.

Purified products of end joining reactions exposed to increasing amounts of nuclease S1 (Fig. 5*B*) are initially resistant to digestion, and when digestion occurs, a smear rather than the original substrate is generated. This is consistent with the absence of nicks at the sites of end joining and suggests that DNA ligase III joins both DNA strands when it forms higher order multimers.

Because the purified products tested in the above experiment were formed after a 1-hour end joining, it was possible that double-stranded joining occurred in two steps, well separated in time, each involving the independent joining of DNA single strands. To test this possibility, we allowed DNA end joining for periods of time between 2 and 20 minutes and tested nuclease S1 digestion of the products. We reasoned that if two, timely well-separated events, lead to the double strand DNA joining, the digestibility of the products will be high after short periods of incubation when only one of the two ligation events is likely to have taken place.

In these experiments, nuclease S1 treatment followed end joining without product purification and was initiated by first adding acetate to the end joining reaction mixture to establish optimal pH for nuclease S1 function, followed by incubation at 37°C for 30 minutes. In separate control experiments, we established that addition of acetate completely stops DNA end joining and that the substrate specificity of nuclease S1 is not altered by the components of the end joining buffer. Figure 5*C* shows the results of a typical experiment. There is no increased nuclease S1 sensitivity even when digestibility is tested after 2 minutes of end joining.

As a further test, end joining efficiency was measured in reactions where nuclease S1 up to 1 unit was included during the end joining reaction and was therefore able to act immediately after the first rejoining step, albeit under suboptimal digestion conditions. There was no detectable effect on the efficiency of end joining under these conditions, and higher concentrations of nuclease S1 (up to 100 units) only generated nonspecific substrate degradation (data not shown).

To examine whether the above indicated resistance of the DNA end joining products to nuclease S1 is partly due to traces of protein remaining bound on DNA after purification from the gel and despite treatment with proteinase E, we purified DNA from end joining reactions using phenol/chloroform extraction followed by ethanol precipitation. Subsequently, we separated the products from unligated substrate by gel electrophoresis and tested their nuclease S1 sensitivity. The results (not shown) are similar to those shown in Fig. 5*B* and indicate that blocking of the end joining site by remaining protein cannot be invoked to explain the observed resistance to nuclease S1.

The above results in aggregate are compatible with DNA ligase III joining the two strands of the DNA substrate during multimer production either simultaneously, or with a temporal separation of <1 minute; it therefore can be considered as being practically simultaneous.

Knock down of *LIG3* in *LIG4*$^{-/-}$ mouse embryo fibroblasts compromises DNA end joining. The biochemical experiments described above suggest a role for DNA ligase III in the rejoining of DNA DSBs. Because DNA-PK–dependent end joining is thought to depend exclusively on DNA ligase IV, we postulated that DNA ligase III functions in backup pathways of NHEJ, such as B-NHEJ. To experimentally test this possibility, we introduced a plasmid DNA end joining assay similar to the one employed in the biochemical experiments described above but developed for direct reporting *in vivo* over EGFP expression (21). Because the dominance of DNA ligase IV *in vivo* was expected to make it difficult to discern a role for DNA ligase III in wild type cells, we designed these experiments using *LIG4*$^{-/-}$ MEF (17). We reasoned that in the absence of DNA

ligase IV, the dependence of DNA end joining on DNA ligase III would be more pronounced and that it could be experimentally shown by RNAi.

Figure 6*A* shows the pEGFP-Pem1-Ad2 plasmid used in the experiments (21). The plasmid is linearized by *Hin*dIII digestion that removes, when complete on both sides, the Ad2 exon and enables upon successful intracellular circularization EGFP expression that can be detected and quantitated by flow cytometry. Supercoiled pEGFP-Pem1 plasmid is used to evaluate the EGFP signal without requirement for rejoining, whereas the pDsRed2-N1 is used as transfection control. Figure 6*B*, *panel 1* shows the autofluorescence of sham-transfected cells, whereas panels 2 and 3 the green and red fluorescence detected 24 hours after transfection with 0.2 μg pEGFP-Pem1, or 0.2 μg pDsRed2-N1, respectively. These flow cytometry measurements, which were carried out under the conditions outlined in Materials and Methods, allowed the setting of the indicated gates for the quantitative analysis of the following end joining results. Signals generated in cells transfected with both plasmids simultaneously and measured 24 hours later are shown in panel 4.

When *LIG4*$^{-/-}$ MEF are transfected with linearized pEGFP-Pem1-Ad2, the signal shown in Fig. 6*C*, *panel 3* is obtained. Although reduced compared with the signal generated by an equal amount of supercoiled pEGFP-Pem1 (*Panel 1*) it is clearly detectable suggesting considerable end joining efficiency in the absence of DNA ligase IV activity. To evaluate the contribution of DNA ligase III in this reaction, *LIG4*$^{-/-}$ MEF were treated with *LIG3* siRNA. The Western blot in Fig. 6*D* indicates efficient knock down of DNA ligase III to about 20% of *LIG4*$^{-/-}$ MEF treated with a control siRNA sequence. Whereas the knock down efficiency varied from experiment to experiment, we consistently observed reductions in DNA ligase III level between 50% to 80%.

Whereas expression of EGFP from supercoiled pEGFP-Pem1 was not affected by treatment with *LIG3* siRNA (Fig. 6*C*, *panel 2*), the signal obtained with an equal amount of linearized pEGFP-Pem1-Ad2 was reduced by nearly 70% compared with cells treated with control siRNA (Fig. 6*C*, *panel 4* and Fig. 6*D*). In four independent experiments, a reduction in end joining between 40% and 70% was observed that correlated with the levels of DNA ligase III knock down in each of the experiments (50-80%). These results in aggregate provide direct support for an *in vivo* function of DNA ligase III in DSB end joining.

Discussion

The results described above identify DNA ligase III as the main activity contributing to the joining of plasmid DNA ends in extracts of HeLa and 180BR cells. Several observations support this conclusion: DNA ligase III fractionates with the maximum of DNA end joining activity through two columns and its immunodepletion causes a practically complete inhibition of

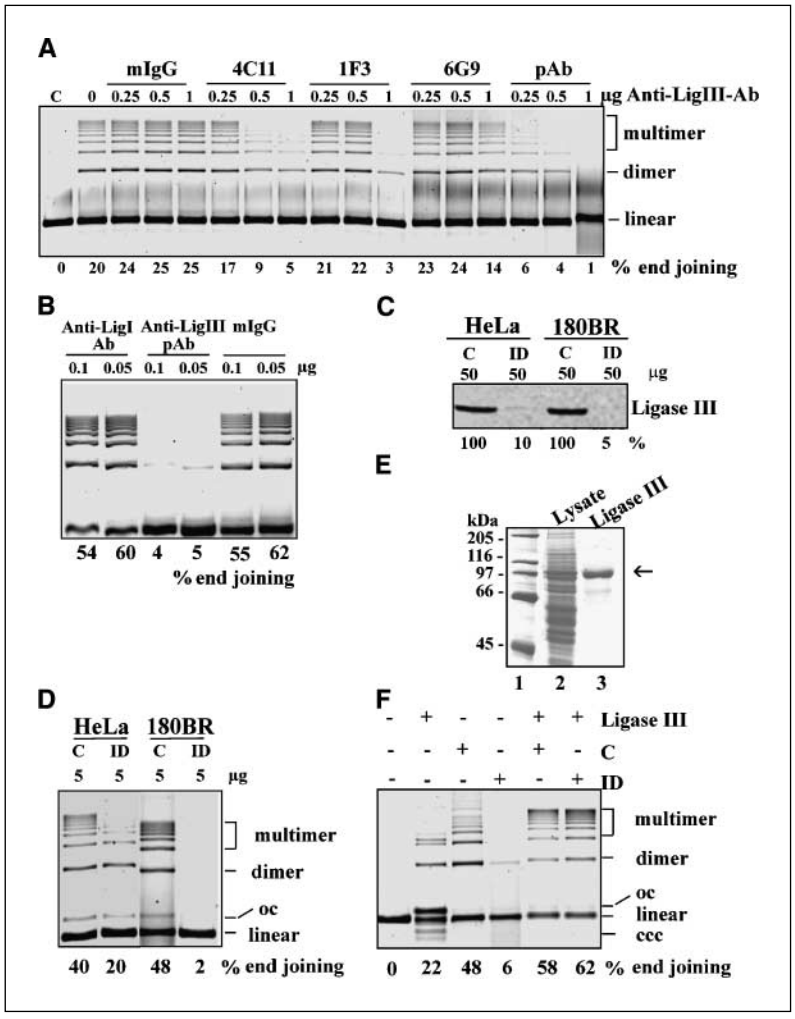

Figure 4. DNA ligase III is involved *in vitro* DNA end joining. *A,* the effect of antibodies raised against human DNA ligase III (4C11, 1F3, 6G9, pAb) was tested in DNA end joining reactions assembled with 10 μg HeLa WCE. Antibodies at the indicated amounts were incubated for 10 minutes at 25°C in 10 μL NHEJ buffer and all reaction components, except DNA and ATP. Subsequently, 10 μL of the same buffer containing 0.25 μg of substrate DNA and 2 mmol/L ATP were added to start the reaction. End joining was allowed to take place for 1 hour at 25°C. mIgG indicates an unrelated antibody used as control. The numbers at the bottom of the gel indicate percent end joining. *B,* similar to (*A*) but for WCE from 180BRM cells (10 μg). In addition to the mouse polyclonal antibody raised against human DNA ligase III (pAb), an unrelated antibody (mIgG) and a monoclonal antibody raised against DNA ligase I were tested. Other details as in (*A*). *C,* Western blot of control and DNA ligase III immunodepleted (*ID*) extracts used in the reactions shown in (*D*). 50 μg of control (*C*) or immunodepleted extracts were loaded on 10% SDS-PAGE and probed with anti–ligase III serum. DNA ligase III is undetectable in immunodepleted extract of 180BR cells, and only a faint band can be seen in ID extracts of HeLa cells. *D,* DNA end joining activity of DNA ligase III depleted HeLa or 180BRM WCE. Reactions were assembled with 5 μg of extract depleted either with an unrelated mouse IgG (*C*), or with the anti–DNA ligase III polyclonal antibody (pAb; *ID*). Other details as in (*A*). *E,* Coomassie-stained gel with purified DNA Ligase III (*lane 3*). For comparison, the initial sf9 cell extract is shown on *lane 2* and size markers on *lane 1*. *F,* Purified recombinant human DNA ligase IIIβ restores DNA end joining activity in immunodepleted 180BRM WCE (10 μg). DNA end joining reactions were assembled with 20 ng purified DNA ligase III (*lane 2*), 10 μg of control extract (*C*, *lane 3*), 10 μg of immunodepleted extract (*lane 4*), 10 μg of control and 20 ng of purified DNA ligase III (*lane 5*), or 10 μg of immunodepleted and 20 ng of purified DNA ligase III (*lane 6*). Other details as in Fig. 1.

DNA end joining that is restored by purified, recombinant enzyme. In addition, the loss of end joining activity in crude cell extracts dialyzed in low salt buffers seems caused by precipitation of DNA ligase III (Fig. 1*A*). Interestingly, the dependence of DNA end joining on DNA ligase III holds not only in the few fractions containing exclusively this ligase activity but also in the crude extracts, where other DNA ligase activities are present and could contribute to the overall effect.

The biological significance of these biochemical observations is corroborated by the *in vivo* results obtained using EGFP rescue in *LIG4*$^{-/-}$ MEF. The 70% reduction in end joining activity after treatment with siRNA is in line with an involvement of this DNA ligase in DSB repair and makes it an excellent candidate factor for backup pathways of NHEJ.

Although DNA ligase III is predominantly considered a component of single-strand break and base excision repair, where it interacts with XRCC1, PARP-1, and pol β (20, 31–34), our observations hint to a potential role in DNA DSB rejoining as well. The resistance of the reaction products to nuclease S1 after only minutes of end joining excludes simple SSB rejoining as the process leading to their formation. Thus, DNA ligase III may be a *bona fide* component of DNA DSB repair by NHEJ, where it may function either alone or together with XRCC1 and PARP-1. This is in line with the ability of the purified enzyme to ligate plasmid DNA under physiologic conditions (35–37) and is directly supported by recent *in vivo* and *in vitro* results (38). Backup pathways of NHEJ operating independently of DNA ligase IV were also suggested by recent genetic experiments in *Drosophila melanogaster* and shown involved in the repair of DSBs induced either after exposure to radiation, or after excision of a P element on a DmRad51-deficient genetic background (39). Evidence is thus mounting that NHEJ pathways operating independently of DNA-PK and DNA ligase IV operate in a variety of organisms (5, 7, 25, 40–42). The results presented here and those of the recent report by Audebert et al. (38) further suggest potential role of DNA ligase III in these backup pathways.

Earlier reports have also provided circumstantial evidence for an involvement of DNA ligase III in DNA DSB rejoining. Fractionation of *Xenopus* extracts identified DNA ligase III in an active fraction, devoid of DNA-PK, that promoted an error-prone, microhomology-driven form of NHEJ (43). These observation suggests similar roles for this ligase in a variety of organisms from *Xenopus* to man. In addition, reduction of DNA ligase III levels by antisense technology in human tumor cells reduces by 78% the DNA end joining activity of the corresponding extracts (37, 44), in line with a role of DNA ligase III in DNA end joining under *in vitro* conditions. Furthermore, a mitochondrial form of DNA ligase III has been documented in human cells (44) and in *Xenopus laevis* oocytes (45) operating independently of XRCC1 (46) and synthesized from an alternative initiation site on the *LIG3* cDNA. This form of DNA ligase III is the only detectable DNA ligase activity in the mitochondria of higher eukaryotes and its down regulation with anti sense oligonucleotides reduces DNA end joining activity in mitochondria extracts (37, 47).

The above summarized observations corroborate our results and indicate that DNA ligase III plays a dominant role in DNA DSB rejoining *in vitro*, thus implying essential functions *in vivo* as well. Because *in vivo* DNA ligase IV is an integral component of the dominant DNA-PK–dependent pathway of NHEJ, D-NHEJ, DNA ligase III is likely to be involved in backup pathways such as B-NHEJ. However, because backup pathways of NHEJ may be suppressed by D-NHEJ (5, 7), the contribution of DNA ligase III in the process may not be easily discernible in cells with wild-type levels of D-NHEJ function. This probably explains why studies in cells with reduced levels of DNA ligase III, such as the EM9 mutant, fail to show reduced rejoining of DNA DSBs (48, 49). In addition, in our *in vivo* experiments, a clear inhibition of DNA end joining after *LIG3* knock down could only be documented in *LIG4*$^{-/-}$ MEF (Fig. 6).

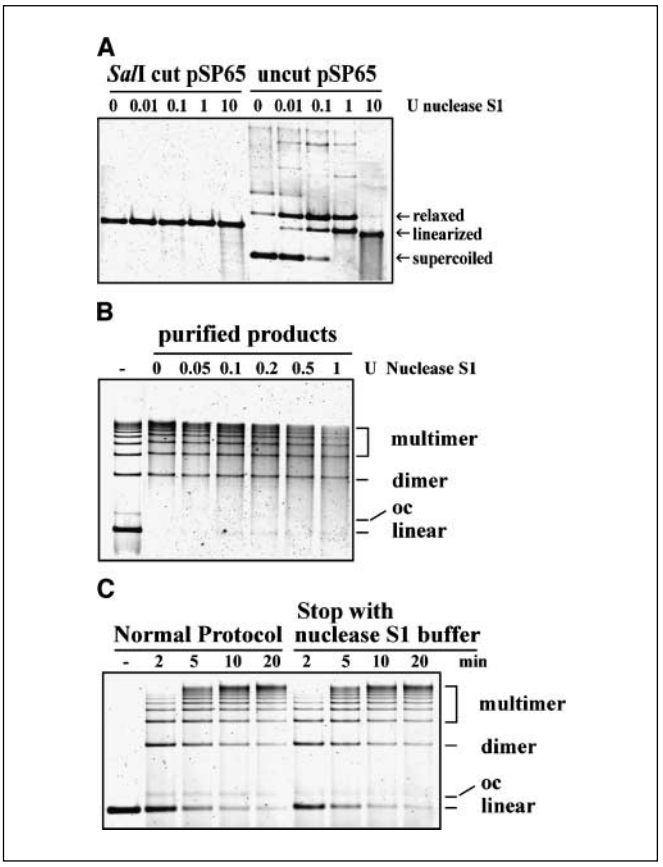

Figure 5. Product formation during DNA end joining involves the ligation of both strands of the DNA substrate. *A,* the specificity of nuclease S1. *Sal*I cut pSP65 plasmid (250 ng, used as substrate for DNA end joining) and uncut pSP65 plasmid were incubated for 30 minutes at 37°C with increasing amount of nuclease S1 and separated by gel electrophoresis (see Materials and Methods). *B,* products of the reaction (*first lane*) were purified from a preparative gel and incubated with increasing amounts of nuclease S1 for 30 minutes at 37°C. Reaction products were examined by gel electrophoresis. *C,* incubation with different amounts of nuclease S1 of DNA end joining reactions that were allowed to proceed for the indicated periods of time. DNA end joining was either stopped using the standard protocol (left), or with nuclease S1 buffer (pH 4.5; *right*). The latter set of reactions was subsequently incubated for 30 minutes at room temperature with 1 unit nuclease S1 and treated with proteinase E, 0.5% SDS, and EDTA before fractionation by agarose gel electrophoresis.

The dominance of DNA ligase III in DNA end joining *in vitro* is noteworthy vis-à-vis the dominance of DNA ligase IV under *in vivo* conditions and raises several important questions. It is not obvious by what mechanism a ligase with such dominant activity in DNA end joining *in vitro* relinquishes this dominant position to DNA ligase IV *in vivo*. This is particularly intriguing because DNA ligase III maintains dominance in DNA end joining even when other components of D-NHEJ such as DNA-PKcs, Ku, and XRCC4 are present in the extract and are, therefore, able to interact and cooperate with DNA ligase IV. Furthermore, the inhibitory effects of wortmannin and anti-Ku antibodies *in vitro* (5, 7) suggest that

these NHEJ factors exert at least partly their expected activities in DNA end joining, yet without detectably impeding the function of DNA ligase III. The simplest interpretation of this apparent discrepancy, that also considers the limitations of the *in vitro* assay, is that DNA ligase IV and the associated D-NHEJ factors operate optimally in the context of chromatin rather than in free DNA in solution. We have proposed a model in which the juxtaposition of DNA ends generated as a result of the DSB in the context of chromatin is invoked to explain the high efficiency of D-NHEJ *in vivo*, as well as some of the discrepancies in the kinetic characteristics between main and backup pathways *in vivo* and *in vitro* (5, 6, 41). This chromatin based explanation is in line with the function of DNA ligase III in back-up pathways of NHEJ that have also been suggested from results obtained *LIG4*$^{-/-}$ DT40 cells (50).

The involvement of DNA ligase III in backup pathways of NHEJ does not only explain residual DNA DSB rejoining in cells with defects in DNA ligase IV but also hints to the possible involvement of DNA ligase III interacting proteins such as PARP-1 in the process. Indeed, there is circumstantial evidence for the involvement of PARP-1 in DNA DSB rejoining (51, 52), but this involvement could not be conclusively and universally shown (53–55). However, if the role of PARP-1 is limited to a contribution in backup pathways of NHEJ, it is easy to see why this contribution will be difficult to detect for as long as the primary pathways of end joining remain active. In addition, competition with other DNA lesions may mask this contribution when damage is induced by agents such as ionizing radiation that induce on top of DSBs over an order of magnitude more single-strand breaks and base damages that need to be repaired by the same system. Recent results suggest an involvement of PARP-1 in conjunction with DNA ligase III in the rejoining of DSB (38), but a specific contribution to backup pathways of NHEJ has not been formally shown. It remains to be established how the balance between the DNA ligase IV and DNA ligase III–dependent pathways of NHEJ is maintained in the cell nucleus. Addressing these questions will likely be a fruitful area for future research.

Mammalian cells show an extraordinary ability to join transfected DNA maintained extrachromosomally, either by direct ligation or by using microhomologies (56, 57). Our *in vivo* results (Fig. 6) suggest that in the absence of DNA ligase IV and probably also of D-NHEJ in general, this rejoining relies to a significant degree on DNA ligase III. Such involvement of DNA ligase III can explain the efficient end joining of transfected DNA in cells deficient in DNA-PKcs (12, 58, 59), Ku (12, 60), XRCC4 (12, 60), or DNA ligase IV (12) and may help to understand the observed preference in the use of microhomologies in some of these mutants (12, 60). It is also possible that *in vitro* experiments implicating Ku in the fidelity of end joining, as well as in the inhibition of the pathway using microhomologies (12, 18, 61, 62) have been carried

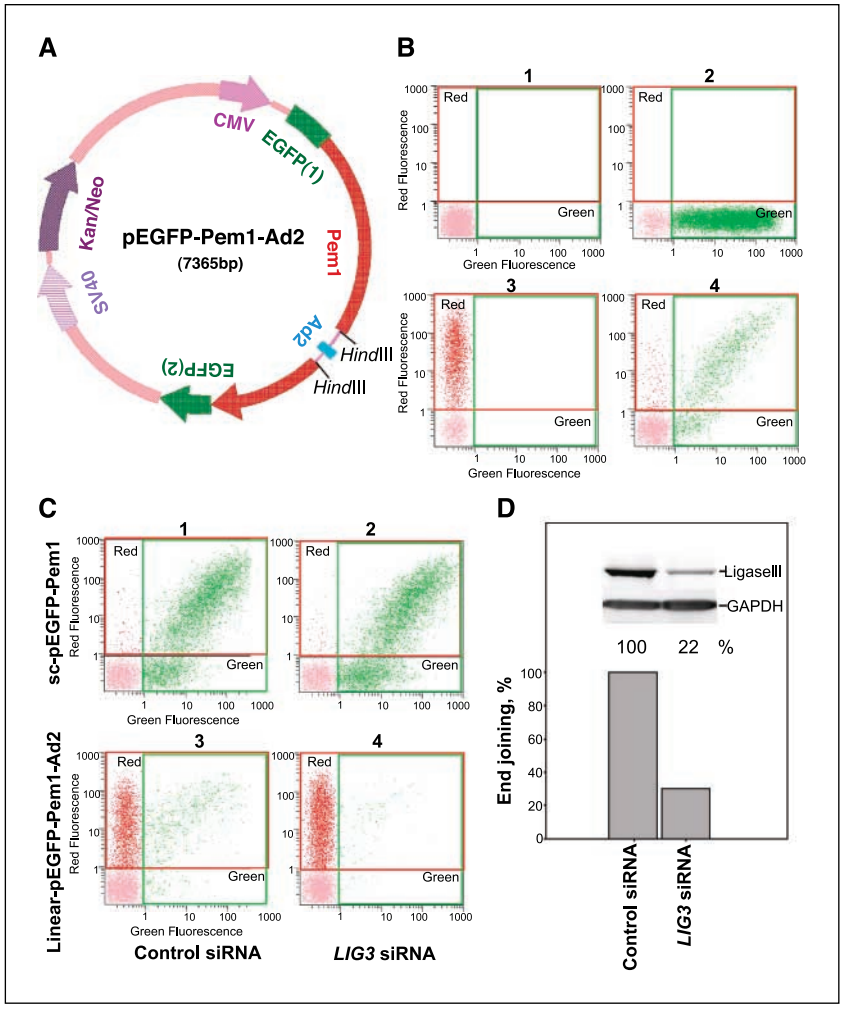

Figure 6. DNA ligase III contributes to DNA end joining *in vivo*. *A,* map of pEGFP-Pem1-Ad2. Note the Pem1 intron, the Ad2 exon and the location of the *Hin*dIII cutting sites (see Materials and Methods for details). *B,* dot plots of nontransfected LIG4$^{-/-}$ MEF (*1*), MEF transfected with 0.2 μg pEGFP-Pem1 (*2*), MEFs transfected with 0.2 μg DsRed (*3*), or MEFs transfected with both plasmids together (*4*). *C,* dot plots of LIG4$^{-/-}$ MEFs transfected either with 0.2 μg supercoiled pEGFP-Pem1 (*1* and *2*), or 0.2 μg *Hin*dIII linearized pEGFP-Pem1-Ad2 (*3* and *4*) together with 0.2 μg DsRed. MEF pretreated for 24 hours with control siRNA (*1* and *3*) and MEF pretreated for 24 hours with *LIG3* siRNA (*2* and *4*; S2 sequence; see Materials and Methods). *D,* Western blot for DNA ligase III in cells treated for 24 hours with control or *LIG3* siRNA. Quantitative analysis considering signal intensity of the GAPDH loading control gives for this experiment a knock down effect of 78%. DNA rejoining of linearized pEGFP-Pem1-Ad2 in cells treated for 24 hours with *LIG3* siRNA normalized to that of cells treated with control siRNA. In this experiment, 78% knock down of *LIG3* caused a 70% reduction in the efficiency of rejoining. All measurements of rejoining efficiency were carried out 24 hours after transfection of the corresponding plasmids. Similar results were also obtained 48 hours later.

out under conditions favoring the function of DNA ligase III. Finally, although V(D)J recombination shows a stricter dependence than NHEJ on DNA-PK and DNA ligase IV/XRCC4, it can also use alternative, DNA-PK–independent pathways that rely on microhomologies for the formation of nonstandard V(D)J recombination products (12). To the extent that this form of end joining can occur in the absence of DNA ligase IV, DNA ligase III is a potential candidate.

In summary, the results presented here identify DNA ligase III, which is unique to vertebrates, as the prevailing DNA end joining activity in extracts of human cells and provide direct evidence for a role in DNA end joining *in vivo*. Although this activity is inherent to the enzyme, it has not been unequivocally identified before in extracts of mammalian cells despite its significant contribution under optimized conditions of end joining. These observations raise the possibility that DNA ligase III functions *in vivo* in a backup pathway of DNA end joining (B-NHEJ), removing DNA DSBs when D-NHEJ is either inactive or unable to function. The dominance of DNA ligase III in DNA end joining *in vitro* is intriguing vis-à-vis the dominance of DNA ligase IV under *in vivo* conditions, and indicates that components of the D-NHEJ apparatus may have been optimized for function in the context of chromatin. Further genetic models will elucidate the potential role of DNA ligase III in backup pathways of NHEJ and will differentiate these backup pathways from of subpathways of D-NHEJ using DNA ligase IV (23, 24).

Acknowledgments

Received 8/23/2004; revised 2/18/2005; accepted 3/24/2005.

Grant support: Volkswagenstiftung; and Deutsche Forschungsgemeinschaft; European Commission Contract FIGH-CT-2002-00217; NIH, Department of Health and Human Services grants RO1 CA42026 and RO1 CA56706; IFORES program of the University of Duisburg-Essen; and NIH, National Cancer Institute, Department of Health and Human Services grant T32 CA09137 (H. Wang).

The costs of publication of this article were defrayed in part by the payment of page charges. This article must therefore be hereby marked *advertisement* in accordance with 18 U.S.C. Section 1734 solely to indicate this fact.

We thank Drs. E.P. Malaise (Inserm Unit 247, Institut Gustave-Roussy, Villejuif, France) and C.F. Arlett (MRC Cell Mutation Unit, Sussex University, Brighton, United Kingdom) for kindly providing the 180BR cells, Dr. F. Alt (Howard Hughes Medical Institute, The Children's Hospital, Boston, MA) for kindly providing the *LIG4*$^{-/-}$ MEFs, Dr. Harvey Ozer for the pRNS-1 plasmid, L. Li (University of Texas, M.D. Anderson Cancer Center, Houston, TX) for providing the pEGFP-Pem1, V. Gorbunova (University of Rochester, Rochester, NY) for providing pEGFP-Pem1-Ad2, Dr. A. Tomkinson (Department of Molecular Medicine, Institute of Biotechnology, the University of Texas health Science Center, San Antonio, Texas) for the generous gift of DNA ligase III expression vector and purified protein for initial experiments, and Dr. S.P. Jackson (Department of Zoology, Cambridge University, Cambridge, United Kingdom) for anti-Ligase IV and anti-XRCC4 antibodies.

References

1. Valerie K, Povirk LF. Regulation and mechanisms of mammalian double-strand break repair. Oncogene 2003; 22:5792–812.
2. Thompson LH, Limoli CL. Origin, recognition, signaling, and repair of DNA double-strand breaks in mammalian cells. In: Caldecott K, editor. Eukaryotic DNA damage surveillance and repair. Landes Press. Chapter 6, p. 107-45. Available from: http://www.landesbioscience.com.
3. Jackson SP. Sensing and repairing DNA double-strand breaks. Carcinogenesis 2002;23:687–96.
4. Dynan WS, Yoo S. Interaction of ku protein and DNA-dependent protein kinase catalytic subunit with nucleic acids. Nucleic Acids Res 1998;26:1551–9.
5. Wang H, Perrault AR, Takeda Y, Qin W, Wang H, Iliakis G. Biochemical evidence for Ku-independent backup pathways of NHEJ. Nucleic Acids Res 2003;31:5377–88.
6. Iliakis G, Wang H, Perrault AR, et al. Mechanisms of DNA double strand break repair and chromosome aberration formation. Cytogenet Genome Res 2004;104: 14–20.
7. Perrault R, Wang H, Wang M, Rosidi B, Iliakis G. Backup pathways of NHEJ are suppressed by DNA-PK. J Cell Biochem 2004;92:781–94.
8. Zhu C, Mills KD, Ferguson DO, et al. Unrepaired DNA breaks in p53-deficient cells lead to oncogenic gene amplification subsequent to translocations. Cell 2002; 109:811–21.
9. Gao Y, Ferguson DO, Xie W, et al. Interplay of p53 and DNA-repair protein XRCC4 in tumorigenesis, genomic stability and development. Nature 2000;404: 897–900.
10. Difilippantonio MJ, Zhu J, Chen HT, et al. DNA repair protein Ku80 suppresses chromosomal aberrations and malignant transformation. Nature 2000;404:510–4.
11. Lee GS, Neiditch MB, Salus SS, Roth DB. RAG proteins shepherd double-strand breaks to a specific pathway, suppressing error-prone repair, but RAG nicking initiates homologous recombination. Cell 2004;117:171–84.
12. Verkaik NS, Esveldt-van Lange REE, van Heemst D, et al. Different types of V(D)J recombination and end-joining defects in DNA double-strand break repair mutant mammalian cells. Eur J Immunol 2002; 32:701–9.
13. Plowman PN, Bridges BA, Arlett CF, Hinney A, Kingston JE. An instance of clinical radiation morbidity and cellular radiosensitivity, not associated with ataxia-telagiectasia. Br J Radiol 1990;63:624–8.
14. Riballo E, Critchlow SE, Teo S-H, et al. Identification of a defect in DNA ligase IV in a radiosensitive leukaemia patient. Curr Biol 1999;9:699–702.
15. Riballo E, Doherty AJ, Dai Y, et al. Cellular and biochemical impact of a mutation in DNA ligase IV conferring clinical radiosensitivity. J Biol Chem 2001; 276:31124–32.
16. Badie C, Iliakis G, Foray N, et al. Induction and rejoining of DNA double-strand breaks and interphase chromosome breaks after exposure to X rays in one normal and two hypersensitive human fibroblast cell lines. Radiat Res 1995;144:26–35.
17. Frank KM, Sharpless NE, Gao Y, et al. DNA ligase IV deficiency in mice leads to defective neurogenesis and embryonic lethality via the p53 pathway. Mol Cell 2000; 5:993–1002.
18. Labhart P. Ku-dependent nonhomologous DNA end joining in *Xenopus* egg extracts. Mol Cell Biol 1999;19: 2585–93.
19. Tomkinson AE, Roberts E, Daly G, Totty NF, Lindahl T. Three distinct DNA ligases in mammalian cells. J Biol Chem 1991;266:21728–35.
20. Mackey ZB, Niedergang C, Menissier-de Murcia J, et al. DNA ligase III is recruited to DNA strand breaks by a zinc finger motif homologous to that of poly (ADP-ribose) polymerase. J Biol Chem 1999;274:21679–87.
21. Seluanov A, Mittelman D, Pereira-Smith OM, Wilson JH, Gorbunova V. DNA end joining becomes less efficient and more error-prone during cellular senescence. Proc Natl Acad Sci U S A 2004;101:7624–9.
22. Baumann P, West SC. DNA end-joining catalyzed by human cell-free extracts. Proc Natl Acad Sci U S A 1998; 95:14066–70.
23. Udayakumar D, Bladen CL, Hudson FZ, Dynan WS. Distinct pathways of nonhomologous end joining that are differentially regulated by DNA-dependent protein kinase-mediated phosphorylation. J Biol Chem 2003; 278:41631–5.
24. Lee K-J, Jovanovic M, Udayakumar D, Bladen CL, Dynan WS. Identification of DNA-PKcs phosphorylation sites in XRCC4 and effects of mutations at these sites on DNA end joining in a cell-free system. DNA Repair 2004;3:267–76.
25. Wang H, Zhao-Chong Z, Perrault AR, Cheng X, Qin W, Iliakis G. Genetic evidence for the involvement of DNA ligase IV in the DNA-PK-dependent pathway of nonhomologous end joining in mammalian cells. Nucleic Acids Res 2001;29:1653–60.
26. Levin DS, Bai W, Yao N, O'Donnell M, Tomkinson AE. An interaction between DNA ligase I and proliferating cell nuclear antigen: implications for Okazaki fragment synthesis and joining. Proc Natl Acad Sci U S A 1997; 94:12863–8.
27. Taylor AM, Whitehouse CJ, Cappelli E, Frosina G, Caldecott KW. Role of DNA ligase III zinc finger in polynucleotide binding and ligation. Nucleic Acids Res 1998;26:4804–10.
28. Timson DJ, Singleton MR, Wigley DB. DNA ligases in the repair and replication of DNA. Mutat Res 2000;460: 301–18.
29. Tomkinson AE, Mackey ZB. Structure and function of mammalian DNA ligases. Mutat Res 1998;407:1–9.
30. Tomkinson A, Levin DS. Mammalian DNA ligases. BioEssays 1997;19:893–901.
31. Caldecott KW, McKeown CK, Tucker JD, Ljungquist S, Thompson LH. An interaction between the mammalian DNA repair protein XRCC1 and DNA ligase III. Mol Cell Biol 1994;14:68–76.
32. Caldecott K, Tucker JD, Stanker LH, Thompson LH. Characterization of the XRCC1-DNA ligase III complex *in vitro* and its absence from mutant hamster cells. Nucleic Acids Res 1995;23:4836–43.
33. Caldecott KW, Aoufouchi S, Johnson P, Shall S. XRCC1 polypeptide interacts with DNA polymerase β and possibly poly (ADP-ribose) polymerase, and DNA ligase III is a novel molecular "nick-sensor" *in vitro*. Nucleic Acids Res 1996;24:4387–94.
34. Cappelli E, Taylor R, Cevasco M, Abbondandolo A, Caldecott K, Frosina G. Involvement of XRCC1 and DNA ligase III gene products in DNA base excision repair. J Biol Chem 1997;272:23970–5.
35. Taylor AM, Whitehouse CJ, Caldecott KW. The DNA ligase III zinc finger stimulates binding to DNA secondary structure and promotes endjoining. Nucleic Acids Res 2000;28:3558–63.
36. Chen L, Trujillo K, Sung P, Tomkinson AE. Interactions of the DNA ligase IV-XRCC4 complex with DNA ends and the DNA-dependent protein kinase. J Biol Chem 2000;275:26196–205.
37. Lakshmipathy U, Campbell C. Double strand break rejoining by mammalian mitochondrial extracts. Nucleic Acids Res 1999;27:1198–204.

38. Audebert M, Salles B, Calsou P. Involvement of poly(ADP-ribose) polymerase-1 and XRCC1/DNA ligase III in an alternative route for DNA double-strand breaks rejoining. J Biol Chem 2004;279:55117–26.

39. McVey M, LaRocque JR, Adams MD, Sekelsky JJ. Formation of deletions during double-strand break repair in *Drosophila* DmBlm mutants occurs after strand invasion. Proc Natl Acad Sci U S A 2004;101:15694–9.

40. Cheong N, Perrault AR, Wang H, et al. DNA-PK-independent rejoining of DNA double-strand breaks in human cell extracts *in vitro*. Int J Radiat Biol 1999;75: 67–81.

41. DiBiase SJ, Zeng Z-C, Chen R, Hyslop T, Curran WJ Jr, Iliakis G. DNA-dependent protein kinase stimulates an independently active, nonhomologous, end-joining apparatus. Cancer Res 2000;60:1245–53.

42. Wang H, Zeng Z-C, Bui T-A, et al. Efficient rejoining of radiation-induced DNA double-strand breaks in vertebrate cells deficient in genes of the RAD52 epistasis group. Oncogene 2001;20:2212–24.

43. Goettlich B, Reichenberger S, Feldmann E, Pfeiffer P. Rejoining of DNA double-strand breaks *in vitro* by single-strand annealing. Eur J Biochem 1998;258:387–95.

44. Lakshmipathy U, Campbell C. The human DNA ligase III gene encodes nuclear and mitochondrial proteins. Mol Cell Biol 1999;19:3869–76.

45. Perez-Jannotti RM, Klein SM, Bogenhagen DF. Two forms of mitochondrial DNA ligase III are produced in *Xenopus laevis* oocytes. J Biol Chem 2001;276:48978–87.

46. Lakshmipathy U, Campbell C. Mitochondrial DNA ligase III function is independent of Xrcc1. Nucleic Acids Res 2000;28:3880–6.

47. Lakshmipathy U, Campbell C. Antisense-mediated decrease in DNA ligase III expression results in reduced mitochondrial DNA integrity. Nucleic Acids Res 2001;29: 668–76.

48. Thompson LH, Brookman KW, Jones NJ, Allen SA, Carrano AV. Molecular cloning of the human XRCC1 gene, which corrects defective DNA strand break repair and sister chromatid exchange. Mol Cell Biol 1990;10: 6160–71.

49. van Ankeren SC, Murray D, Stafford PM, Meyn RE. Cell survival and recovery processes in Chinese hamster AA8 cell and in two radiosensitive clones. Radiat Res 1988;115:223–37.

50. Adachi N, Ishino T, Ishii Y, Takeda S, Koyama H. DNA ligase IV-deficient cells are more resistant to ionizing radiation in the absence of Ku70: implications for DNA double-strand break repair. Proc Natl Acad Sci U S A 2001;98:12109–13.

51. Süsse S, Scholz C-J, Bürkle A, Wiesmüller L. Poly(ADP-ribose) polymerase (PARP-1) and p53 independently function in regulating double-strand break repair in primate cells. Nucleic Acids Res 2004;32:669–80.

52. Rudat V, Bachmann N, Küpper J-H, Weber K-J. Overexpression of the DNA-binding domain of poly(ADP-ribose) polymerase inhibits rejoining of ionizing radiation-induced DNA double-strand breaks. Int J Radiat Biol 2001;77:303–7.

53. Noel G, Giocanti N, Fernet M, Megnin-Chanet F, Favaudon V. Poly(ADP-ribose) polymerase (PARP-I) is not involved in DNA double-strand break recovery. BMC Cell Biol 2003;4:7–16.

54. D'Amours D, Desnoyers S, D'Silva I, Poirier GG. Poly(ADP-ribosyl)ation reactions in the regulation of nuclear functions. Biochem J 1999;342:249–68.

55. Yang Y-G, Cortes U, Patnaik S, Jasin M, Wang Z-Q. Ablation of PARP-1 does not interfere with the repair of DNA double-strand breaks, but compromises the reactivation of stalled replication forks. Oncogene 2004;23:3872–82.

56. Roth DB, Porter TM, Wilson JH. Mechanisms of nonhomologous recombination in mammalian cells. Mol Cell Biol 1985;5:2599–607.

57. Roth DB, Wilson JH. Nonhomologous recombination in mammalian cells: role for short sequence homologies in the joining reaction. Mol Cell Biol 1986; 6:4295–304.

58. Chang C, Biedermann KA, Mezzina M, Brown JM. Characterization of the DNA double strand break repair defect in scid mice. Cancer Res 1993;53:1244–8.

59. Harrington J, Hsieh CL, Gerton J, Bosma G, Lieber MR. Analysis of the defect in DNA end joining in the murine scid mutation. Mol Cell Biol 1992;12:4758–68.

60. Kabotyanski EB, Gomelsky L, Han J-O, Stamato TD, Roth DB. Double-strand break repair in Ku86- and XRCC4-deficient cells. Nucleic Acids Res 1998;26: 5333–42.

61. Feldmann E, Schmiemann V, Goedecke W, Reichenberger S, Pfeiffer P. DNA double-strand break repair in cell-free extracts from Ku80-deficient cells: implications for Ku serving as an alignment factor in non-homologous DNA end joining. Nucleic Acids Res 2000;28:2585–96.

62. Chen S, Inamdar KV, Pfeiffer P, et al. Accurate *in vitro* end joining of a DNA double strand break with partially cohesive 3′-overhangs and 3′-phosphoglycolate termini. Effect of Ku on repair fidelity. J Biol Chem 2001;276: 24323–30.